Analytical study of the amplitude and phase resonances of a Duffing oscillator

M. Volvert, G. Kerschen
University of Liège, Department of Aerospace and Mechanical Engineering,
Space Structures and Systems Laboratory (S3L)
Quartier Polytech 1 (B52/3), Allée de la Découverte 9, Liege, B-4000, Belgium

Abstract
This paper revisits the resonant behavior of a harmonically-forced Duffing oscillator with a specific attention to phase resonance and to its relation with amplitude resonance. To this end, the different families of resonances, namely primary (1:1), superharmonic (k:1) and subharmonic (1:ν) resonances are carefully studied using first and higher-order averaging. When the phase lag is calculated between the k-th harmonic of the displacement and the harmonic forcing, this study evidences that phase resonance occurs when the phase lag is equal to either $\pi/2$ (phase quadrature) or $3\pi/4\nu$.

1 Introduction

The resonant behavior of linear systems can be characterized either with the concept of an amplitude resonance or a phase resonance. Amplitude resonance corresponds to a relative maximum in the frequency response function whereas phase resonance is associated with quadrature between the displacement and the external forcing. At phase resonance, the external forcing cancels exactly the damping force with the result that the resonance frequency coincides with the natural frequency of the linear system. The difference between the two resonances remains small for weakly damped systems. Phase resonance-based testing [1] which excites the individual modes of the system in turn was largely exploited during the early days of experimental modal analysis because it provides accurate estimation of the modal parameters. With the advent of advanced system identification techniques such as the stochastic subspace identification method [2], phase resonance testing has been less and less employed for linear modal analysis.

For nonlinear systems, the phase lag quadrature criterion was first extended to synchronous motions using harmonic balance in [3] and then to arbitrary periodic motions using Melnikov analysis in [4]. These efforts triggered the development of nonlinear phase resonance testing which targets the identification of the nonlinear normal modes (NNMs) defined as periodic solutions of the unforced, undamped system [5, 6]. Basic [7, 8, 9] and more advanced (control-based) strategies [10, 11, 12, 13, 14, 15] were developed during the last decade. In this context, phase-locked loops (PLLs) are particularly effective for tracking phase quadrature for increasing forcing amplitudes, as first proposed in [11]. In addition, like control-based continuation [10], phase control may also stabilize unstable periodic solutions.

Despite the great promise of PLLs for experimental modal analysis of nonlinear systems, two difficulties remain for an accurate and thorough characterization of nonlinear resonant behaviors. First, according to [3], the correspondence between the quadrature curves identified using PLLs and NNMs is only valid for multiharmonic forcing. In the presence of modal interactions, the discrepancy can be very important [16]. Second, nonlinear systems can exhibit additional resonances including superharmonic and subharmonic resonances. Even if recent theoretical [4] and numerical [17] studies investigated these secondary resonances under the banner of nonlinear modes, it is not yet fully clear how they can be identified using phase resonance testing.

To provide a solid theoretical framework for the use of PLLs in nonlinear experimental modal analysis, the present study revisits the resonant behavior of a harmonically-forced Duffing oscillator with a specific attention to phase resonance and to its relation with amplitude resonance. To this end, the different families

of resonances including primary (1:1), superharmonic (k:1) and subharmonic (1:ν) resonances are carefully studied using first and higher-order averaging.

The paper is organized as follows. Section 2 briefly recalls the principles behind averaging in nonlinear dynamics. Section 3 focuses on the amplitude and phase resonances of both a linear and a Duffing oscillator whereas Section 4 extends the investigations to different secondary resonances. In Section 5, the findings obtained through the analytical derivations are verified using numerical simulations. The conclusions of the present study are summarized in Section 6.

2 General approach

2.1 Resonances of a Duffing oscillator

The governing equation of motion of a mass-normalized and harmonically-forced Duffing oscillator is

$$\ddot{x}(t) + 2\bar{\zeta}\,\omega_0\,\dot{x}(t) + \omega_0^2 x(t) + \alpha x^3(t) = \bar{\gamma}\sin\omega t \tag{1}$$

where $\bar{\zeta}$ is the linear modal damping ratio, α is the nonlinear stiffness coefficient, $\bar{\gamma}$ is the forcing amplitude whereas ω is the excitation frequency of period T. The natural frequency of the undamped, linearized system is ω_0 [18]. The Duffing oscillator is said to be hardening when $\alpha > 0$, and softening when $\alpha < 0$. In the present study, we set $\bar{\zeta} = 0.005$, $\omega_0 = 1$ and $\alpha = 1$. Thus, only the hardening case is studied here.

If we consider the Fourier decomposition of the displacement

$$x(t) = A_0 + \sum_{k=1}^{n} A_k \sin\left(\omega_k t - \phi_k\right) \tag{2}$$

where $\omega_k = \frac{k\omega}{\nu}$ (with ν a positive integer), A_k and ϕ_k are the frequency, amplitude and phase lag of the k-th harmonic of the displacement, respectively, then Equation (2) shows that each harmonic k may trigger a resonance if ω_k corresponds to the (amplitude-dependent) frequency of the primary resonance of the system. These resonances can be divided into four categories, namely $1:1$ primary resonance ($k = \nu = 1$), $k:1$ superharmonic resonances, $1:\nu$ subharmonic resonances and $k:\nu$ ultra-subharmonic resonances.

2.2 Averaging around the $k:\nu$ resonance

We consider a weakly nonlinear oscillator of the form:

$$\ddot{x}(t) + \omega_0^2 x(t) = \varepsilon f(x(t), \dot{x}(t)) \tag{3}$$

When $\varepsilon = 0$, the periodic solution of (3) is written as:

$$x(t) = u\cos\omega_0 t - v\sin\omega_0 t \tag{4}$$

where u and v are constants. When $\varepsilon \neq 0$, we seek a solution of frequency ω_k such that ${\omega_k}^2 - {\omega_0}^2 = \varepsilon\,\Omega$. The solution is expressed as in Equation (4) but with time-dependent u and v:

$$x(t) = u(t)\cos\omega_k t - v(t)\sin\omega_k t \tag{5}$$

We impose that the velocity should have the same form as in the case $\varepsilon = 0$, *i.e.*,

$$\dot{x}(t) = -u(t)\,\omega_k \sin\omega_k t - v(t)\,\omega_k \cos\omega_k t \tag{6}$$

Equation (6) holds if:

$$\dot{u}(t)\cos\omega_k t - \dot{v}(t)\sin\omega_k t = 0 \tag{7}$$

Differentiating Equation (6) and replacing $\ddot{x}(t)$ and $x(t)$ in Equation (3) yields:

$$\dot{u}(t)\,\omega_k \sin\omega_k\,t + \dot{v}(t)\,\omega_k \cos\omega_k\,t = -\varepsilon\left[f(x(t),\dot{x}(t)) + \Omega\,x(t)\right] \tag{8}$$

Finally, taking into account Equations (7) and (8) and solving for $\dot{u}$ and $\dot{v}$, a system of first-order equations is obtained:

$$\begin{cases} \dot{u} = -\frac{\varepsilon}{\omega_k}\left[f(x(t),\dot{x}(t)) + \Omega\,x(t)\right]\sin\omega_k\,t \\ \dot{v} = -\frac{\varepsilon}{\omega_k}\left[f(x(t),\dot{x}(t)) + \Omega\,x(t)\right]\cos\omega_k\,t \end{cases} \tag{9}$$

This system has a suitable form to apply first- or higher-order averaging. First-order averaging is performed herein using the Krylov-Bogolyubov technique [19, 20]. Higher-order averaging is based on the Lie transform algorithm [20]; it was implemented by Yagasaki in the *haverage.m* Mathematica package [21].

$x(t)$ is often represented using the polar coordinates r and ϕ such that $x(t) = r(t)\sin(\omega\,t - \phi(t))$ with $r = \sqrt{u^2+v^2}$ and $\phi = \mathrm{atan2}(-u,-v)$. For conciseness, the time dependence for u, v, r and ϕ is dropped in the remainder of this article.

3 Primary resonance ($k = \nu = 1$)

Considering Equation (1), we scale the system such that $\bar{\zeta} = \varepsilon\zeta$ and $\bar{\gamma} = \varepsilon^{3/2}\gamma$, with ζ, $\gamma = \mathcal{O}(1)$. If $x = \sqrt{\varepsilon}y$, we obtain:

$$\ddot{y}(t) + 2\varepsilon\zeta\,\omega_0\,\dot{y}(t) + \omega_0^2 y(t) + \varepsilon\alpha y^3(t) = \varepsilon\gamma\sin\omega t \tag{10}$$

The forcing frequency is in the vicinity of the natural frequency of the linear system, i.e., $\omega^2 - {\omega_0}^2 = \varepsilon\Omega$. The displacement is expressed as:

$$x(t) = \sqrt{\varepsilon}r\sin(\omega\,t - \phi) = A\sin(\omega\,t - \phi) \tag{11}$$

3.1 Linear system

Applying first-order averaging to the linear system ($\alpha = 0$) yields:

$$\begin{cases} \dot{r} = -\frac{\varepsilon}{\omega}\left(2\zeta\,\omega_0\,\omega\,r - \gamma\sin\phi\right) \\ \dot{\phi} = \frac{\varepsilon}{\omega}\left(\Omega + \gamma\cos\phi\right) \end{cases} \tag{12}$$

Assuming a steady-state response, *i.e.*, $\dot{r} = \dot{\phi} = 0$, the motion around resonance is governed by:

$$\begin{cases} 2\zeta\,\omega_0\,\omega\,r = \gamma\sin\phi \\ -\Omega\,r = \gamma\cos\phi \end{cases} \tag{13}$$

The resonant behavior of a linear oscillator can be described in two different ways, i.e., either when the amplitude of the frequency response undergoes a relative maximum (i.e., amplitude resonance denoted by a subscript *a* herein) or when the displacement is in quadrature with the external forcing (i.e., phase resonance denoted by a subscript *p*). Both cases are detailed in what follows.

3.1.1 Phase lag at amplitude resonance

Amplitude resonance occurs when both $\frac{\partial r}{\partial\,\omega}$ and $\frac{\partial r}{\partial\phi}$ are equal to 0. From Equation (13), we obtain:

$$\begin{cases} \frac{\partial r}{\partial\phi} = \frac{\gamma}{2\zeta\,\omega_0\,\omega}\left(\cos\phi - \frac{\sin\phi}{\omega}\frac{\partial\,\omega}{\partial\phi}\right) = 0 \\ \frac{\partial r}{\partial\,\omega} = \frac{\gamma}{2\zeta\,\omega_0\,\omega}\left(\cos\phi\frac{\partial\phi}{\partial\,\omega} - \frac{\sin\phi}{\omega}\right) = 0 \end{cases} \tag{14}$$

Both relations are equivalent. The second relation of Equations (13) provides an expression for ω:

$$\omega = \sqrt{{\omega_0}^2 - \frac{\varepsilon\gamma}{r}\cos\phi} \tag{15}$$

$\frac{\partial\omega}{\partial\phi}$ is obtained by isolating Ω in the second equation of (13) and making use of the chain rule $\frac{\partial\omega}{\partial\phi} = \frac{\partial\omega}{\partial\Omega}\frac{\partial\Omega}{\partial\phi}$ such that

$$\frac{\partial\,\omega}{\partial\phi} = \frac{\varepsilon}{2\,\omega}\left(\frac{\gamma}{r}\sin\phi + \frac{\gamma}{r^2}\cos\phi\frac{\partial r}{\partial\phi}\right) \tag{16}$$

which can be inserted in the first relation of (14):

$$\frac{\partial r}{\partial\phi} = \frac{\gamma\sin\phi}{2\zeta\,\omega_0\,\omega}\frac{(\omega - \varepsilon\zeta\,\omega_0\tan\phi)}{(\omega\tan\phi + \varepsilon\zeta\,\omega_0)} = 0 \tag{17}$$

This relationship is satisfied when the phase lag takes the form:

$$\tan\phi_a = \frac{\omega_a}{\varepsilon\zeta\,\omega_0} = \frac{\sqrt{1-2\bar{\zeta}^2}}{\bar{\zeta}} \tag{18}$$

The corresponding frequency and amplitude are

$$\omega_a = \omega_0\sqrt{1-2\bar{\zeta}^2},\quad A_a = \frac{\bar{\gamma}}{2\bar{\zeta}\,{\omega_0}^2\sqrt{1-\bar{\zeta}^2}} \tag{19}$$

It should be noted that $\phi = 0$ or $\phi = \pi$ also verify Equation (17) and correspond to the purely static and inertial responses, respectively.

3.1.2 Phase lag at phase resonance

Phase quadrature $\phi_p = \frac{\pi}{2}$ occurs when the excitation frequency corresponds to the natural frequency of the undamped system, i.e., when $\omega = \omega_p = \omega_0$. The amplitude at phase resonance is $A_p = \frac{\bar{\gamma}}{2\bar{\zeta}\,{\omega_0}^2}$.

3.2 Nonlinear system

First-order averaging applied to the nonlinear system ($\alpha \neq 0$) gives:

$$\begin{cases} \dot{r} = -\frac{\varepsilon}{\omega}\left(\zeta\,\omega_0\,\omega\,r - \frac{\gamma}{2}\sin\phi\right) \\ \dot{\phi} = -\frac{\varepsilon}{\omega}\left(\frac{\alpha}{8}\left(3r^2 - \frac{4\,\Omega}{\alpha}\right) - \frac{\gamma}{2}\cos\phi\right) \end{cases} \tag{20}$$

The steady-state solutions around the primary resonance are governed by:

$$\begin{cases} \zeta\,\omega_0\,\omega\,r = \frac{\gamma}{2}\sin\phi \\ \frac{\alpha}{8}\left(3r^2 - \frac{4\,\Omega}{\alpha}\right)r = \frac{\gamma}{2}\cos\phi \end{cases} \tag{21}$$

3.2.1 Phase lag at amplitude resonance

Following the same procedure as for the linear system, we obtain:

$$\begin{cases} \frac{\partial r}{\partial\phi} = \frac{\gamma}{2\zeta\,\omega_0\,\omega}\left(\cos\phi - \frac{\sin\phi}{\omega}\frac{\partial\omega}{\partial\phi}\right) = 0 \\ \frac{\partial r}{\partial\omega} = \frac{\gamma}{2\zeta\,\omega_0\,\omega}\left(\cos\phi\frac{\partial\phi}{\partial\omega} - \frac{\sin\phi}{\omega}\right) = 0 \end{cases} \tag{22}$$

and

$$\frac{\partial\,\omega}{\partial\phi} = \frac{\varepsilon}{2\,\omega}\left(\left[\frac{6\alpha r}{4} + \frac{\gamma}{r^2}\cos\phi\right]\frac{\partial r}{\partial\phi} + \frac{\gamma}{r}\sin\phi\right) \tag{23}$$

Eventually,

$$\frac{\partial r}{\partial\phi} = \frac{8\zeta\,\omega_0\,\omega^2\,\gamma\sin\phi(\omega - \varepsilon\zeta\,\omega_0\tan\phi)}{16\zeta^2\,{\omega_0}^2\,\omega^4\tan\phi + \varepsilon(3\alpha\gamma^2\sin\phi^2\tan\phi + 16\zeta^3\,{\omega_0}^3\,\omega^3)} \tag{24}$$

This relation is verified when:

$$\tan\phi_a = \frac{\omega_a}{\varepsilon\zeta\,\omega_0} \tag{25}$$

and, from (21) and (25), it is possible to derive A_a, ω_a and ϕ_a as a function of the forcing and the system parameters:

$$\begin{cases} A_a = \sqrt{\frac{2\,{\omega_0}^2}{3\alpha}\left((\bar{\zeta}^2 - 1) + \sqrt{(1-\bar{\zeta}^2)^2 + \frac{3\alpha\bar{\gamma}^2}{4\bar{\zeta}^2\,{\omega_0}^6}}\right)} \\ \omega_a = \frac{\omega_0}{\sqrt{2}}\sqrt{1 - 3\bar{\zeta}^2 + \sqrt{\left(1-\bar{\zeta}^2\right)^2 + \frac{3\alpha\bar{\gamma}^2}{4\bar{\zeta}^2\,{\omega_0}^6}}} \\ \tan\phi_a = \frac{\sqrt{1-3\bar{\zeta}^2+\sqrt{\left(1-\bar{\zeta}^2\right)^2+\frac{3\alpha\bar{\gamma}^2}{4\bar{\zeta}^2\,{\omega_0}^6}}}}{\sqrt{2}\bar{\zeta}}. \end{cases} \tag{26}$$

3.2.2 Phase lag at phase resonance

Imposing $\phi_p = \pi/2$ in Equations (21) yields:

$$\begin{cases} A_p = \frac{\bar{\gamma}}{2\bar{\zeta}\,\omega_0\,\omega_p} \\ \omega_p = \omega_0\sqrt{1 + \frac{3\alpha}{4\,{\omega_0}^2}A_p^2} \end{cases} \tag{27}$$

from which the expressions of the amplitude and frequency at phase resonance can be deduced:

$$A_p = \sqrt{\frac{2\,{\omega_0}^2}{3\alpha}\left(\sqrt{1 + \frac{3\alpha\bar{\gamma}^2}{4\bar{\zeta}^2\,{\omega_0}^6}} - 1\right)} \tag{28}$$

and

$$\omega_p = \frac{\omega_0}{\sqrt{2}}\sqrt{1 + \sqrt{1 + \frac{3\alpha\bar{\gamma}^2}{4\bar{\zeta}^2\,{\omega_0}^6}}} \tag{29}$$

We note that Equations (27) correspond to those that would be obtained by applying the energy balance principle [22, 23] to the NNMs of the undamped, unforced system and neglecting higher-order harmonics. Under this latter assumption, this means that phase resonance testing amounts to exciting the underlying NNMs.

3.2.3 Discussion

This section has derived analytical expressions of the amplitude, frequency and phase of a Duffing oscillator at amplitude and phase resonances. Of specific interest is the difference in frequency between amplitude and phase resonances, $\Delta\omega = \omega_p - \omega_a$:

$$\Delta\,\omega = \frac{\omega_0}{\sqrt{2}}\left(\sqrt{1 + \sqrt{1 + \frac{3\alpha\bar{\gamma}^2}{4\bar{\zeta}^2\,{\omega_0}^6}}} - \sqrt{1 - 3\bar{\zeta}^2 + \sqrt{\left(1-\bar{\zeta}^2\right)^2 + \frac{3\alpha\bar{\gamma}^2}{4\bar{\zeta}^2\,{\omega_0}^6}}}\right) \tag{30}$$

We note that the phase resonance of a harmonically-forced Duffing oscillator is rarely discussed in the technical literature. The reason might come from the fact that perturbation techniques do not always make a distinction between amplitude and phase resonances. For example, the method of multiple scales [24] yields around the primary resonance:

$$\begin{cases} \zeta\,{\omega_0}^2\,r = \frac{\gamma}{2}\sin\phi \\ \frac{\alpha}{8}\left(3r^2 - \frac{8\,\omega_0(\omega-\omega_0)}{\varepsilon\alpha}\right) r = \frac{\gamma}{2}\cos\phi \end{cases} \tag{31}$$

Since the amplitude r is maximum when $\phi = \pi/2$, amplitude and phase resonances are predicted to occur simultaneously with:

$$\begin{cases} A = \frac{\bar{\gamma}}{2\bar{\zeta}\,{\omega_0}^2} \\ \omega = \omega_0 + \frac{3\alpha\bar{\gamma}^2}{32\bar{\zeta}^2\,{\omega_0}^5} \end{cases} \tag{32}$$

Interestingly, the multiple scales method predicts that the amplitude at resonance of the Duffing oscillator is identical to that of the phase resonance of the underlying linear system.

Getting back to Equation (30) and performing a Taylor series expansion indicates that the frequency difference is of the order of $\mathcal{O}\left(\bar{\zeta}^2\right)$, as in the linear case. For weak to moderate damping (i.e., not beyond a few percent, which is usually the case for mechanical structures), it thus follows that phase resonance lies in the immediate neighborhood of amplitude resonance. This is illustrated in Figures 1a and 1b, where the phase resonance curve constructed thanks to Equations (28) and (29) is superposed to the nonlinear frequency responses calculated from Equations (21) for different forcing amplitudes. Expression (30) also evidences that a hardening nonlinearity (α>0) brings amplitude and phase resonances closer to each other, and conversely for a softening nonlinearity.

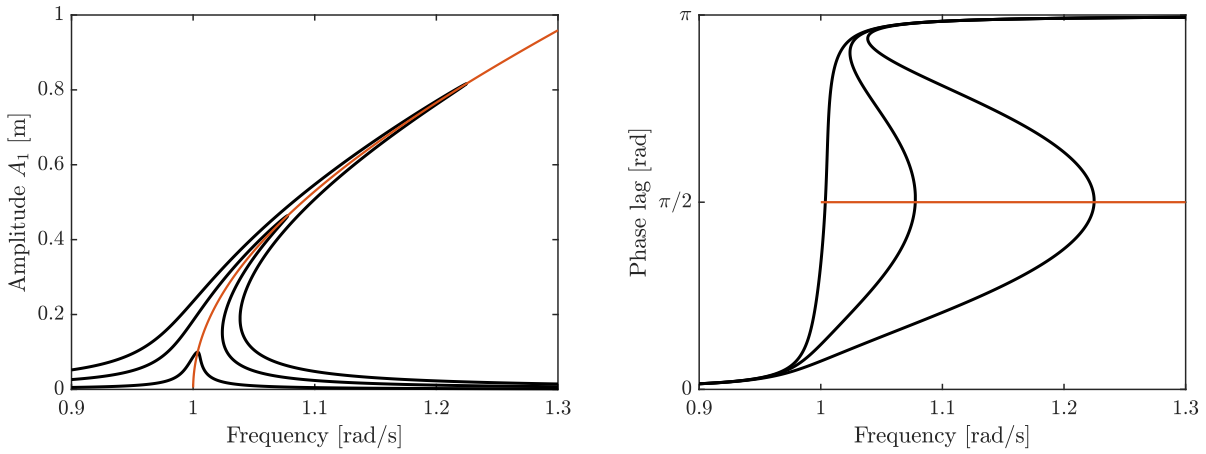

(a) (b)

Figure 1: Nonlinear frequency responses (black) around the primary resonance of the Duffing oscillator for forcing amplitudes of 0.001N, 0.005N and 0.01N and the phase resonance curve (orange): (a) amplitude and (b) phase lag.

4 Secondary resonances

Considering the mass-normalized equation of the Duffing oscillator (1), we scale the system such that $\bar{\zeta} = \varepsilon^d\zeta$ and $\bar{\gamma} = \sqrt{\varepsilon}\gamma$, with μ, $\gamma = \mathcal{O}(1)$, and d is a positive integer. If we let $x = \sqrt{\varepsilon}y$, we obtain

$$\ddot{y}(t) + 2\varepsilon^d\zeta\,\omega_0\,\dot{y}(t) + \omega_0^2 y(t) + \varepsilon\alpha y^3(t) = \gamma\sin\omega t \tag{33}$$

If $\varepsilon = 0$, then Equation (33) has a periodic solution $y(t) = \Gamma \sin \omega t$ with $\Gamma = \gamma/(\omega_0^2 - \omega^2)$. Introducing $z(t) = y(t) - \Gamma \sin \omega t$ in Equation (33) yields a weakly nonlinear oscillator with a form suitable for first- or higher-order averaging:

$$\ddot{z}(t) + \omega_0^2 z(t) = \varepsilon f(z(t), \dot{z}(t), \omega t, \varepsilon) \tag{34}$$

where

$$f(z(t), \dot{z}(t), \omega t, \varepsilon) = -\alpha(z(t) + \Gamma \sin \omega t)^3 - 2\varepsilon^{d-1} \zeta\, \omega_0 (\dot{z}(t) + \omega \Gamma \cos \omega t) \tag{35}$$

where the forcing frequency is close to a fraction of the natural frequency of the linear system, i.e., ${\omega_k}^2 - {\omega_0}^2 = \varepsilon\, \Omega$. The solution around the $k : \nu$ resonance can therefore be expressed as:

$$x(t) = \sqrt{\varepsilon}\,(r \sin(\omega_k\, t - \phi) + \Gamma \sin \omega\, t) = A_k \sin(\omega_k\, t - \phi) + \bar{\Gamma} \sin \omega\, t \tag{36}$$

where $A_k = \sqrt{\varepsilon} r$ and $\bar{\Gamma} = \bar{\gamma}/(\omega_0^2 - \omega^2)$.

4.1 $3 : 1$ resonance

The first secondary resonance studied is the $3 : 1$ superharmonic resonance, *i.e.*, $k = 3$ and $\nu = 1$. Using Equation (33) with $d = 1$, first-order averaging provides:

$$\begin{cases} \dot{r} = -\varepsilon \left(\zeta\, \omega_0\, r - \frac{\alpha \Gamma^3}{24\, \omega} \sin \phi \right) \\ \dot{\phi} = -\varepsilon \left(\frac{\alpha}{24\, \omega} \left(3r^2 + 6\Gamma^2 - \frac{4\,\Omega}{\alpha} \right) - \frac{\alpha \Gamma^3}{24\, \omega\, r} \cos \phi \right) \end{cases} \tag{37}$$

Assuming a steady-state solution, $\dot{r} = \dot{\phi} = 0$, we have:

$$\begin{cases} \frac{24 \zeta\, \omega_0\, \omega}{\alpha} r = \Gamma^3 \sin \phi \\ \left(3r^2 + 6\Gamma^2 - \frac{4\,\Omega}{\alpha} \right) r = \Gamma^3 \cos \phi \end{cases} \tag{38}$$

4.1.1 Phase lag at amplitude resonance

As for the primary resonance, amplitude resonance for the $3 : 1$ resonance occurs when $\frac{\partial r}{\partial \omega} = \frac{\partial r}{\partial \phi} = 0$:

$$\begin{cases} \frac{\partial r}{\partial \phi} = \frac{\alpha \Gamma^3}{24 \zeta\, \omega_0\, \omega} \left(\left[\frac{7\,\omega^2 - {\omega_0}^2}{\omega({\omega_0}^2 - \omega^2)} \right] \sin \phi \frac{\partial \omega}{\partial \phi} + \cos \phi \right) = 0 \\ \frac{\partial r}{\partial \omega} = \frac{\alpha \Gamma^3}{24 \zeta\, \omega_0\, \omega} \left(\left[\frac{7\,\omega^2 - {\omega_0}^2}{\omega({\omega_0}^2 - \omega^2)} \right] \sin \phi + \cos \phi \frac{\partial \phi}{\partial \omega} \right) = 0 \end{cases} \tag{39}$$

Isolating Ω from (38), using the chain rule $\frac{\partial \omega}{\partial \phi} = \frac{\partial \omega}{\partial \Omega} \frac{\partial \Omega}{\partial \phi}$ and inserting it in $\frac{\partial r}{\partial \phi}$ gives:

$$\frac{\partial r}{\partial \phi} = \frac{\alpha \Gamma^3 \left(\frac{(7\,\omega^2 - {\omega_0}^2)}{\omega({\omega_0}^2 - \omega^2)} \frac{\varepsilon \zeta\, \omega_0}{3} \sin \phi + \left(1 - \varepsilon \frac{\alpha \Gamma^2}{3({\omega_0}^2 - \omega^2)} + \varepsilon \frac{2 \zeta\, \omega_0\, \omega}{{\omega_0}^2 - \omega^2} \frac{1}{\tan \phi} \right) \cos \phi \right)}{24 \zeta\, \omega_0\, \omega \left(1 - \varepsilon \left(\frac{\alpha \Gamma^2}{3({\omega_0}^2 - \omega^2)} + \frac{2 \zeta\, \omega_0\, \omega}{{\omega_0}^2 - \omega^2} \frac{1}{\tan \phi} - \frac{\alpha^3 \Gamma^3 \sin \phi^2}{6912 \zeta^2\, {\omega_0}^2\, \omega^3} - \frac{\zeta\, \omega_0}{3 \sin \phi \tan \phi} \right) \right)} \tag{40}$$

The numerator is 0 when:

$$\tan^2 \phi - \frac{3\,\omega({\omega_0}^2 - \omega^2)}{\varepsilon \zeta\, \omega_0({\omega_0}^2 - 7\,\omega^2)} \left(1 - \frac{\varepsilon \alpha \Gamma^2}{3({\omega_0}^2 - \omega^2)} \right) \tan \phi - \frac{6\,\omega^2}{({\omega_0}^2 - 7\,\omega^2)} = 0 \tag{41}$$

Solving this equation for $\tan \phi$ and keeping only the leading term, the phase lag at amplitude resonance writes

$$\tan \phi_a = \frac{3\,\omega_a({\omega_0}^2 - \omega_a^2)}{\bar{\zeta}\, \omega_0({\omega_0}^2 - 7\,\omega_a^2)} \tag{42}$$

Assuming further that, since we suppose that ω is close to $\frac{\omega_0}{3}$, the ratio

$$\frac{{\omega_0}^2 - \omega_a^2}{{\omega_0}^2 - 7\,\omega_a^2} \simeq 4 \tag{43}$$

yields:

$$\tan\phi_a = \frac{12\,\omega_a}{\bar{\zeta}\,\omega_0} \tag{44}$$

Inserting this relation in Equations (38) and assuming that the static response is constant, i.e., $\Gamma \simeq \Gamma_* = \frac{9\gamma}{8\,\omega_0}$, provides an expression of the amplitude of the third harmonic and of the frequency at amplitude resonance:

$$\begin{cases} A_{3,a} = \frac{\alpha\bar{\Gamma}_*^3}{2\bar{\zeta}\,{\omega_0}^2\sqrt{\bar{\zeta}^2\,{\omega_0}^2 + 144\,\omega_a^2}} \\ \omega_a = \sqrt{\frac{-c_2+\sqrt{c_2^2-4c_1c_3}}{2c_1}} \end{cases} \tag{45}$$

where

$$\begin{cases} c_1 = \frac{1728}{\alpha} \\ c_2 = -144\left(2\bar{\Gamma}_*^2 + \frac{4\,{\omega_0}^2}{3\alpha} - \frac{3\bar{\zeta}^2}{4\alpha}\right) \\ c_3 = \left(\frac{2\bar{\zeta}^2\,{\omega_0}^2}{3\alpha} - 2\bar{\Gamma}_*^2 - \frac{4\,{\omega_0}^2}{3\alpha}\right)\bar{\zeta}^2\,{\omega_0}^2 - \frac{\alpha^2\bar{\Gamma}_*^6}{4\bar{\zeta}^2\,{\omega_0}^2} \end{cases} \tag{46}$$

4.1.2 Phase lag at phase resonance

For weak to moderate damping, Equation (44) shows that amplitude resonance occurs near phase quadrature between the third harmonic of the displacement and the forcing. The phase resonance for the 3:1 superharmonic resonance can thus be associated with a phase lag of $\pi/2$. The averaged equations of motion (38) become:

$$\begin{cases} r_p = \frac{\alpha\Gamma^3}{24\zeta\,\omega_0\,\omega_p} \\ r_p = \sqrt{\frac{4\,\Omega}{3\alpha} - 2\Gamma^2} \end{cases} \tag{47}$$

If we assume again that $\Gamma \simeq \Gamma_*$, it is possible to derive a closed-form expression for $A_{3,p}$ and ω_p:

$$\begin{cases} A_{3,p} = \frac{\alpha\bar{\Gamma}_*^3}{24\bar{\zeta}\,{\omega_0}^2\,\omega_p^2} \\ \omega_p = \sqrt{\frac{-c_2+\sqrt{c_2^2-4c_1c_3}}{2c_1}} \end{cases} \tag{48}$$

where

$$\begin{cases} c_1 = \frac{1728}{\alpha} \\ c_2 = -144\left(2\bar{\Gamma}_*^2 + \frac{4\,{\omega_0}^2}{3\alpha}\right) \\ c_3 = -\frac{\alpha^2\bar{\Gamma}_*^6}{4\bar{\zeta}^2\,{\omega_0}^2} \end{cases} \tag{49}$$

Figures 2a and 2b compare the nonlinear frequency responses calculated from Equations (38) and the phase resonance curves constructed thanks to Equations (48) and (49). Clearly, the newly-defined concept of a phase resonance for the 3:1 superharmonic resonance is in excellent agreement with the maxima of the third harmonic of the response, at least for the amount of damping considered herein, i.e., 0.5%. Assuming small $\bar{\zeta}$, this observation is also confirmed analytically by the direct comparison between Equations (45)-(46) and (48)-(49).

In the case of a softening Duffing oscillator ($\alpha < 0$), the phase lag ϕ_p should be adjusted to $\frac{3\pi}{2}$ in order to have a positive amplitude $A_{3,p}$. This phase lag is still consistent with Equation (44).

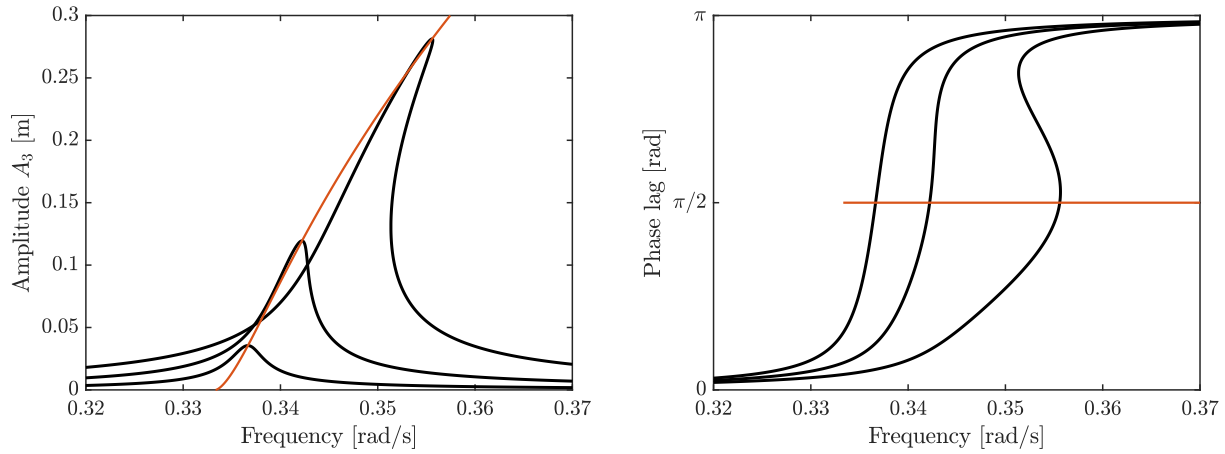

(a) (b)

Figure 2: Nonlinear frequency responses (black) and phase resonance/quadrature curves (orange) around the $3:1$ resonance of the Duffing oscillator for forcing amplitudes of 0.1N, 0.15N and 0.2N: (a) amplitude and (b) phase lag.

4.2 $1:3$ resonance

For the $1:3$ subharmonic resonance, *i.e.*, $k=1$ and $\nu=3$, and $d=1$, first-order averaging gives:

$$\begin{cases} \dot{r} = -\varepsilon\left(\zeta\,\omega_0\,r - \frac{9\alpha\Gamma}{8\,\omega}r^2\sin 3\phi\right) \\ \dot{\phi} = -\varepsilon\left(\frac{3\alpha}{8\,\omega}\left(3r^2+6\Gamma^2-\frac{4\,\Omega}{\alpha}\right) - \frac{9\alpha\Gamma}{8\,\omega}r\cos 3\phi\right) \end{cases} \tag{50}$$

For steady-state solutions,

$$\begin{cases} \zeta\,\omega_0 = \frac{9\alpha\Gamma}{8\,\omega}r\sin 3\phi \\ \frac{3\alpha}{8\,\omega}\left(3r^2+6\Gamma^2-\frac{4\,\Omega}{\alpha}\right) = \frac{9\alpha\Gamma}{8\,\omega}r\cos 3\phi \end{cases} \tag{51}$$

4.2.1 Phase lag at amplitude resonance

Amplitude resonance occurs when $\frac{\partial r}{\partial\omega} = \frac{\partial r}{\partial\phi} = 0$:

$$\begin{cases} \frac{\partial r}{\partial\phi} = \frac{8\zeta\,\omega_0}{9\alpha\Gamma\sin 3\phi}\left(\left(1-\frac{2\,\omega^2}{{\omega_0}^2-\omega^2}\right)\frac{\partial\omega}{\partial\phi} - \frac{3\,\omega}{\tan 3\phi}\right) = 0 \\ \frac{\partial r}{\partial\omega} = \frac{8\zeta\,\omega_0}{9\alpha\Gamma\sin 3\phi}\left(\left(1-\frac{2\,\omega^2}{{\omega_0}^2-\omega^2}\right) - \frac{3\,\omega}{\tan 3\phi}\frac{\partial\phi}{\partial\omega}\right) = 0 \end{cases} \tag{52}$$

We must have $\sin 3\phi \neq 0$, *i.e.*, $\phi \neq \frac{i\pi}{3}$, where i is an integer. Following the same procedure as for the previous resonances gives:

$$\frac{\partial r}{\partial\phi} = \frac{8\zeta\,\omega_0}{9\alpha\Gamma\sin 3\phi}\frac{\left(1-\frac{2\,\omega^2}{{\omega_0}^2-\omega^2}\right)\varepsilon 9\zeta\,\omega_0 - \frac{3\,\omega}{\tan 3\phi}\left(1-\varepsilon\frac{27\alpha\Gamma^2}{{\omega_0}^2-\omega^2}+\varepsilon\frac{6\zeta\,\omega_0}{{\omega_0}^2-\omega^2}\frac{1}{\tan 3\phi}\right)}{1-\varepsilon\frac{27\alpha\Gamma^2}{{\omega_0}^2-\omega^2}+\varepsilon\frac{6\zeta\,\omega_0}{{\omega_0}^2-\omega^2}\frac{1}{\tan 3\phi} - \left(1-\frac{2\,\omega^2}{{\omega_0}^2-\omega^2}\right)\left(\varepsilon\frac{16\zeta^2\,{\omega_0}^2}{3\alpha\Gamma^2\sin^2 3\phi}+\varepsilon\frac{3\zeta\,\omega_0}{\omega\tan 3\phi}\right)} \tag{53}$$

The numerator is equal to 0 when:

$$9\varepsilon\zeta\,\omega_0\left(1-\frac{2\,\omega^2}{{\omega_0}^2-\omega^2}\right)\tan^2 3\phi - 3\,\omega\left(1-\varepsilon\frac{27\alpha\Gamma^2}{{\omega_0}^2-\omega^2}\right)\tan\phi - \varepsilon\frac{18\zeta\,\omega_0\,\omega^2}{{\omega_0}^2-\omega^2} = 0 \tag{54}$$

Solving this equation for $\tan 3\phi$ and keeping only the leading term, the phase lag at amplitude resonance can be approximated with

$$\tan 3\phi_a = \frac{\omega_a}{3\zeta\,\omega_0\left(1+\frac{2\,\omega_a^2}{\omega_a^2-{\omega_0}^2}\right)} \tag{55}$$

Assuming further that, since we suppose that ω is close to $3\,\omega_0$, the ratio

$$\frac{2\,\omega_a^2}{\omega_a^2-{\omega_0}^2} \simeq \frac{9}{4} \tag{56}$$

yields:

$$\tan 3\phi_a = \frac{4\,\omega_a}{39\bar{\zeta}\,\omega_0} \tag{57}$$

Inserting this relation in Equations (51) gives:

$$\begin{cases} A_{1,a} = \frac{2\bar{\zeta}\,\omega_0}{9\alpha\bar{\Gamma}}\sqrt{1521\bar{\zeta}^2\,{\omega_0}^2+16\,\omega_a^2} \\ \bar{\gamma} = \frac{\|\,{\omega_0}^2-\omega_a^2\,\|}{\sqrt{6\alpha}}\sqrt{(2\bar{\Omega}+13\bar{\zeta}^2\,{\omega_0}^2)^2 \pm \sqrt{(2\bar{\Omega}+13\bar{\zeta}^2\,{\omega_0}^2)^2-\frac{8}{9}\bar{\zeta}^2\,{\omega_0}^2(1521\bar{\zeta}^2\,{\omega_0}^2+16\,\omega_a^2)}} \end{cases} \tag{58}$$

where $\bar{\Omega} = \omega_k^2 - {\omega_0}^2$. Unlike the $3:1$ superharmonic resonance, the static response cannot be assumed to be constant because the frequency varies much faster for the 1:3 subharmonic resonance (see Figure 3a). An explicit expression for the resonance frequency ω_a as a function of the forcing $\bar{\gamma}$ can thus not be derived. We also note that, due to the $\pm$ sign, there exist two frequencies satisfying (58), the greatest (lowest) frequency corresponding to the maximum (minimum) response on the isolated branch. It is thus the greatest frequency which is in relation with the resonance frequency ω_a.

4.2.2 Phase lag at phase resonance

For weak to moderate damping, Equation (57) shows that amplitude resonance occurs near phase lags equal to $\frac{\pi}{6}+\frac{i\pi}{3}$ where i is an integer. For odd (even) values of i, r takes positive (negative) values. Considering positive amplitudes, the phase resonance for the 1:3 subharmonic resonance can be associated with phase lags equal to $\frac{\pi}{2}$, $\frac{7\pi}{6}$ and $\frac{11\pi}{6}$. For $\frac{\pi}{2}$, the averaged equations of motion (38) can be transformed into:

$$\begin{cases} A_{1,p} = \frac{8\bar{\zeta}\,\omega_0\,\omega_p}{9\alpha\bar{\Gamma}} \\ \bar{\gamma} = \frac{\|\,{\omega_0}^2-\omega_p^2\,\|}{\sqrt{3\alpha}}\sqrt{\bar{\Omega} \pm \sqrt{\bar{\Omega}^2-\frac{32}{9}\bar{\zeta}^2\,{\omega_0}^2\,\omega_p^2}} \end{cases} \tag{59}$$

The same expressions can be obtained if the two other phase lags are considered instead.

Figures 3a and 3b compare the nonlinear frequency responses calculated from Equations (51) and the phase resonance curve constructed numerically thanks to Equations (59). The phase quadrature curve is found to trace out the locus of the maxima of the different isolated responses.

For a softening Duffing oscillator, amplitude resonance still occurs for phase lags ϕ_p near $\frac{\pi}{6}+\frac{i\pi}{3}$ except that positive amplitudes occur now when i is odd. Thus, the resonant phase lags are $\frac{\pi}{6}$, $\frac{5\pi}{6}$ and $\frac{3\pi}{2}$.

4.3 $1:2$ resonance

Using Equation (33) with $d=2$, second-order averaging yields:

$$\begin{cases} \dot{r} = -\frac{\varepsilon^2}{2}\left(2\zeta\,\omega_0\,r + \frac{33\alpha^2\Gamma^2}{4\,\omega^3}r^3\sin 4\phi\right) \\ \dot{\phi} = -\frac{\varepsilon\alpha}{4\,\omega}\left(3r^2+6\Gamma^2-\frac{4\,\Omega}{\alpha}\right)+\frac{\varepsilon^2}{2}\left(R_{1:2}(r^2)-\frac{33\alpha^2\Gamma^2}{4\,\omega^3}r^2\cos 4\phi\right) \end{cases} \tag{60}$$

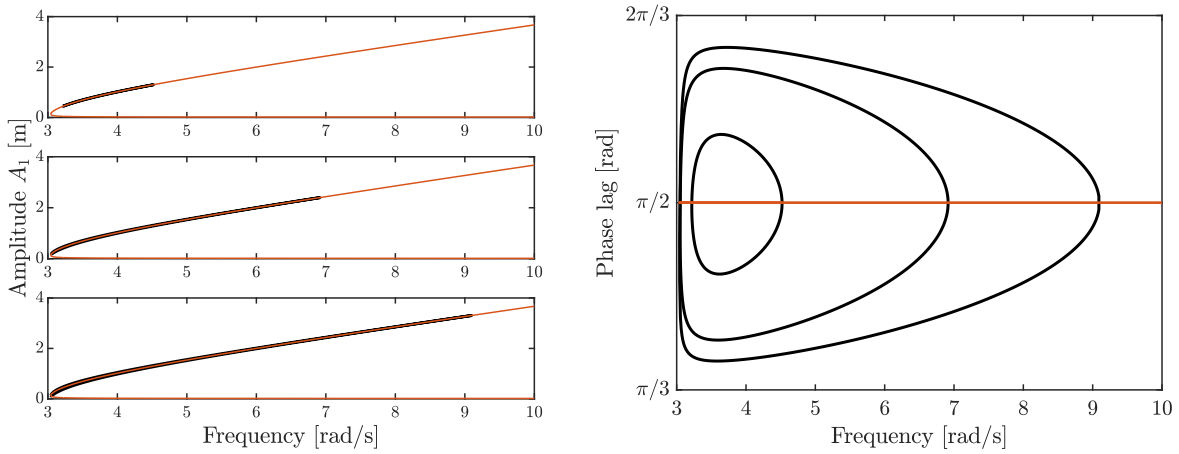

(a) (b)

Figure 3: Nonlinear frequency responses (black) and phase resonance/quadrature curves (orange) around the $1:3$ resonance of the Duffing oscillator for forcing amplitudes of 0.3N, 0.6N and 1N: (a) amplitude and (b) phase lag.

where

$$R_{1:2}(r^2) = \left(\frac{2\,\Omega^2}{\omega^3} - \frac{6\alpha\Gamma^2\,\Omega}{\omega^3} - \frac{51\alpha^2\Gamma^2}{10\,\omega^3}\right) r^2 - \left(\frac{6\alpha\,\Omega}{\omega^3} + \frac{33\alpha^2\Gamma^2}{4\,\omega^3}\right) r^4 + \frac{51\alpha^2}{16\,\omega^3} r^6 \tag{61}$$

Steady-state solutions obey:

$$\begin{cases} 2\zeta\,\omega_0 = -\frac{33\alpha^2\Gamma^2}{4\,\omega^3} r^2 \sin 4\phi \\ \frac{\alpha}{2\,\omega}\left(3r^2 + 6\Gamma^2 - \frac{4\,\Omega}{\alpha}\right) = \varepsilon\left(R_{1:2}(r^2) - \frac{33\alpha^2\Gamma^2}{4\,\omega^3} r^2 \cos 4\phi\right) \end{cases} \tag{62}$$

4.3.1 Phase lag at amplitude resonance

Neglecting the $\mathcal{O}(\varepsilon)$ term in the second Equation of (62) gives an approximation r_0 of the amplitude r:

$$r_0 = \sqrt{\frac{4\,\Omega}{3\alpha} - 2\Gamma^2} \tag{63}$$

Its derivative is:

$$\frac{\partial r_0}{\partial\,\omega} = \frac{4}{r_0}\left(\frac{1}{12\varepsilon\alpha} - \frac{\gamma^2}{({\omega_0}^2 - \omega^2)^3}\right)\omega \tag{64}$$

Considering that the sinus function in the first equation of (62) is bounded by -1 and 1, an existence condition for r is derived:

$$-1 \leq -\frac{8\zeta\,\omega_0\,\omega^3}{33\alpha^2\Gamma^2 r^2} \leq 1 \tag{65}$$

The second inequality is always true. r_0 is thus injected in the first inequality:

$$\frac{4\,\Omega}{3\alpha} \geq 2\Gamma^2 + \frac{8\zeta\,\omega_0\,\omega^3}{33\alpha^2\Gamma^2} \tag{66}$$

The numerical resolution in Figure 4 indicates that, if the forcing exceeds a certain threshold, there exist two frequencies, ω_{inf} and ω_{sup}, which define the domain of existence of the 1:2 subharmonic resonance. Conversely, if the forcing is too low, the inequality is not satisfied, and the 1:2 subharmonic resonance does not exist. Because Equation (64) shows that r_0 is increasing monotonically with respect to frequency since $\alpha > 0$, r_0 is thus maximum (minimum) when ω is equal to ω_{sup} (ω_{inf}), and amplitude resonance occurs

when $\omega = \omega_{sup}$.

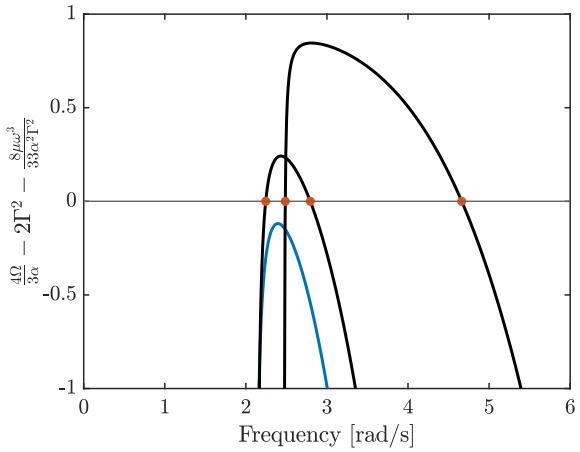

Figure 4: Numerical verification of the inequality (66) for a forcing of 0.8N (blue), 1N and 3N (black).

4.3.2 Phase lag at phase resonance

For this specific resonance, because the $\mathcal{O}(\varepsilon)$ term was neglected in Equations (62), phase resonance corresponds to amplitude resonance and takes place when $\omega = \omega_{sup}$ or, equivalently, $\sin 4\phi_a = -1$. Phase resonance is thus defined for a phase lag $\phi_a = \frac{3\pi}{8} + \frac{i\pi}{2}$, where $i = 0, 1, 2, 3$, which transforms (62) into:

$$\begin{cases} r_p = \sqrt{\frac{8\zeta\,\omega_0\,\omega^3}{33\alpha^2\Gamma^2}} \\ r_p = \sqrt{\frac{4\,\Omega}{3\alpha} - 2\Gamma^2} \end{cases} \tag{67}$$

from which the forcing γ can be computed as a function of the resonant frequency ω_p:

$$\begin{cases} A_p = \sqrt{\frac{8\bar{\zeta}\,\omega_0\,\omega_p^3}{33\alpha^2\bar{\Gamma}^2}} \\ \bar{\gamma} = \frac{\|\,{\omega_0}^2 - \omega_p^2\,\|}{\sqrt{3\alpha}} \sqrt{\bar{\Omega} \pm \sqrt{\bar{\Omega}^2 - \frac{12}{11}\bar{\zeta}\,\omega_0\,\omega_p^3}} \end{cases} \tag{68}$$

The $\pm$ sign indicates that, for a fixed forcing, there exist two possible frequencies corresponding to the minimum and maximum values of A_p.

Figures 5a and 5b compare the nonlinear frequency responses calculated from Equations (62) and the phase resonance curve constructed numerically thanks to Equations (68). The phase resonance curve is found to trace out the locus of the maxima and minima of the different isolated branches.

5 Numerical validation

The analytical results in the previous sections, as well as those found in [25] for higher-order $k : \nu$ resonances, considered the amplitude and phase lag of the harmonic k, i.e., the harmonic triggering the $k : \nu$ resonance. We observed that amplitude resonance was occurring near a well-defined phase lag, allowing us to extend the concept of a phase resonance to secondary resonances. The phase resonances of the Duffing oscillator can be classified into two families depending on the value ϕ_k:

- $\phi_k = \frac{\pi}{2}$ (phase quadrature) when k and ν are odd;
- $\phi_k = \frac{3\pi}{4\nu}$ when either k or ν is even.

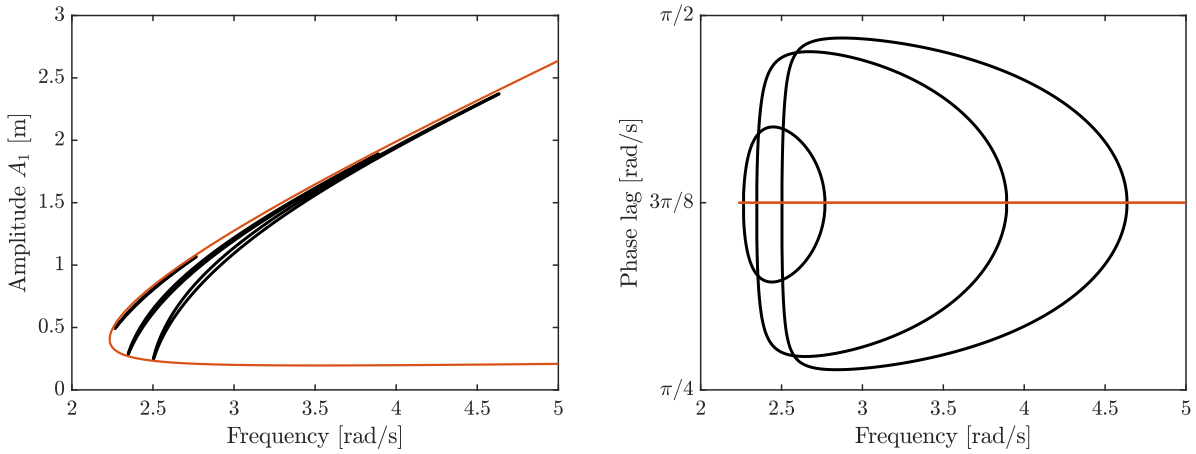

Figure 5: Nonlinear frequency responses (black) and phase resonance curves (orange) around the $1:2$ resonance of the Duffing oscillator for forcing amplitudes of 1N, 2N and 3N: (a) amplitude and (b) phase lag.

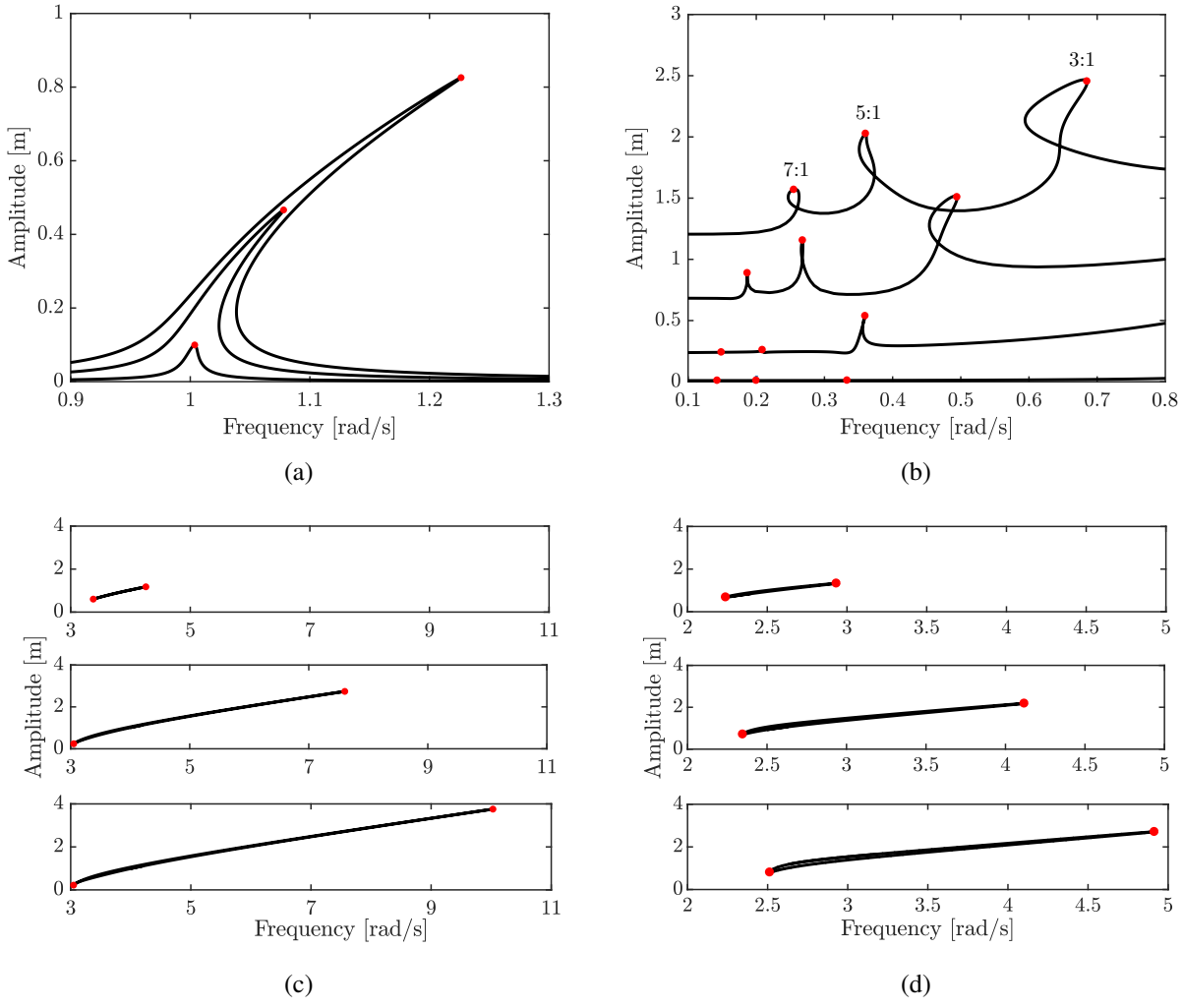

Figure 6: NFRCs (black) and the corresponding phase resonance points (red) of the (a) $1:1$, (b) $k:1$, (c) $1:3$ and (d) $1:2$ resonances.

Though the averaging technique does not give satisfying results for the even superharmonic resonances, their resonant phase lag follows the above rule, i.e., they take the value $\frac{3\pi}{4}$, as evidenced numerically in [17].

To further validate the relevance of our developments, Figure 6 represents the nonlinear frequency responses of the Duffing oscillator calculated numerically using the harmonic balance method [26] for the $1:1$, $3:1$, $5:1$, $7:1$, $1:2$ and $1:3$ resonances. Unlike the previous figures, Figure 6 depicts the multi-harmonic response of the Duffing oscillator. The red dots are located where phase resonance of the k-th harmonic occurs, *i.e.*, $\phi_k = \frac{\pi}{2}$ for the $1:1$, $k:1$ and $1:3$ resonances and $\frac{3\pi}{8}$ for the $1:2$ resonance. We can clearly see that the so-defined phase resonance points can also accurately capture the amplitude resonance of the multi-harmonic response, and not only of the k-th harmonic.

6 Conclusion

The key contribution of this paper is the analytical characterization of the resonant phase lags of a hardening Duffing oscillator. For the $k:\nu$ resonance, the phase lag is computed between the k-th harmonic of the displacement and the harmonic forcing. When k and ν are odd, phase resonance occurs when phase quadrature is achieved. When either k or ν is even, phase resonance takes place for a phase lag equal to $3\pi/4\nu$. In almost all cases considered, phase resonance appears in the immediate vicinity of the amplitude resonance of the kth harmonic, at least for the amount of damping considered in this study.

These analytical results are in complete agreement with the numerical observations made in [17]. They thus confirm the relevance of the concept of a phase resonance nonlinear mode (PRNM) which was defined as the point on the nonlinear frequency response which fulfills the phase resonance conditions. Eventually, the two papers lay down the foundations for rigorous phase resonance testing of nonlinear systems using phase-locked loops [11] and the subsequent correlation between numerical and experimental analyses.

Future work should generalize these results to other types on nonlinearities, including softening nonlinearities, and to higher-dimensional systems.

References

[1] J. Wright, J. Cooper, and M. Desforges, "Normal-mode force appropriation - theory and applications," *Mechanical Systems and Signal Processing*, vol. 13, pp. 217–240, 1999.

[2] P. V. Overschee and B. D. Moor, *Subspace Identification for Linear Systems*. Kluwer Academic Publishers, 1996.

[3] M. Peeters, G. Kerschen, and J. Golinval, "Dynamic testing of nonlinear vibrating structures using nonlinear normal modes," *Journal of Sound and Vibration*, vol. 330, pp. 486–509, 2011.

[4] M. Cedenese and G. Haller, "How do conservative backbone curves perturb into forced responses? a melnikov function analysis," *Proceedings of the Royal Society A*, vol. 476, p. 20190494, 2020.

[5] A. Vakakis, L. Manevitch, Y. Mikhlin, V. Pilipchuk, and A. Zevin, *Normal Modes and Localization in Nonlinear Systems*. John Wiley & Sons, New York, 1996.

[6] G. Kerschen, M. Peeters, J. Golinval, and A. Vakakis, "Nonlinear normal modes, part i: A useful framework for the structural dynamicist," *Mechanical Systems and Signal Processing*, vol. 23, pp. 170–194, 2009.

[7] M. Peeters, G. Kerschen, and J. Golinval, "Modal testing of nonlinear vibrating structures based on nonlinear normal modes: experimental demonstration," *Mechanical Systems and Signal Processing*, vol. 25, pp. 217–240, 2011.

[8] J. Londono, S. Neild, and J. Cooper, "Identification of backbone curves of nonlinear systems from resonant decay responses," *Journal of Sound and Vibration*, vol. 348, pp. 224–238, 2015.

[9] D. Ehrhardt and M. Allen, "Measurement of nonlinear normal modes using multi-harmonic stepped force appropriation and free decay," *Mechanical Systems and Signal Processing*, vol. 76-77, pp. 612–633, 2016.

[10] L. Renson, A. Gonzalez-Buelga, D. Barton, and S. Neild, "Robust identification of backbone curves using control-based continuation," *Journal of Sound and Vibration*, vol. 367, pp. 145–158, 2015.

[11] S. Peter, M. Scheel, M. Krack, and R. Leine, "Synthesis of nonlinear frequency responses with experimentally extracted nonlinear modes," *Mechanical Systems and Signal Processing*, vol. 101, pp. 498–515, 2018.

[12] M. Scheel, S. Peter, R. Leine, and M. Krack, "A phase resonance approach for modal testing of structures with nonlinear dissipation," *Journal of Sound and Vibration*, vol. 435, pp. 56–73, 2018.

[13] T. Karaagacli and N. Ozguven, "Experimental modal analysis of nonlinear systems by using response-controlled stepped-sine testing," *Mechanical Systems and Signal Processing*, vol. 146, p. 107023, 2021.

[14] M. Scheel, "Nonlinear modal testing of damped structures: Velocity feedback vs. phase resonance," *Mechanical Systems and Signal Processing*, vol. 165, p. 108305, 2022.

[15] G. Abeloos, F. Muller, F. Ferhatoglou, M. Scheel, C. Collette, G. Kerschen, M. Brake, P. Tiso, L. Renson, and M. Krack, "A consistency analysis of phase-locked loop testing and control-based continuation using a geometrically nonlinear frictional system," *Mechanical Systems and Signal Processing*, vol. 165, p. 108305, 2022.

[16] L. Renson, T. Hill, D. Ehrhardt, D. Barton, and S. Neild, "Force appropriation of nonlinear structures," *Proceedings of the Royal Society A: Mathematical, Physical, and Engineering Sciences*, vol. 474, p. 20170880, 2018.

[17] M. Volvert and G. Kerschen, "Phase resonance nonlinear modes of mechanical systems," *Journal of Sound and Vibration*, vol. 511, p. 116355, 2021.

[18] I. Kovacic and M. J. Brennan, Eds., *The Duffing Equation: Nonlinear Oscillators and Their Behaviour*. John Wiley & Sons, Hoboken, 2011.

[19] N. Krylov and N. Bogolyubov, *Introduction to non-linear mechanics*. Princeton University Press, 1947.

[20] A. H. Nayfeh, *Perturbation methods*. John Wiley & Sons, New York, 1973.

[21] K. Yagasaki, "Higher-order averaging and ultra-subharmonics in forced oscillators," *J. Sound Vib.*, vol. 210, no. 4, pp. 529–553, 1998.

[22] T. L. Hill, A. Cammarano, S. A. Neild, and D. J. Wagg, "Interpreting the forced responses of a two-degree-of-freedom nonlinear oscillator using backbone curves," *Journal of Sound and Vibration*, vol. 349, pp. 276–288, 2015.

[23] Y. Sun, A. Vizzaccaro, J. Yuan, and L. Salles, "An extended energy balance method for resonance prediction in forced response of systems with non-conservative nonlinearities using damped nonlinear normal mode," *Nonlinear Dynamics*, vol. 103, p. 3315–3333, 2021.

[24] A. H. Nayfeh and D. T. Mook, *Nonlinear oscillations*. John Wiley & Sons, New York, 1995.

[25] M. Volvert and G. Kerschen, "Resonant phase lags of a duffing oscillator," *International Journal of Nonlinear Mechanics (under review arXiv:2202.07556)*, 2022.

[26] T. Detroux, L. Masset, L. Renson, and G. Kerschen, "The harmonic balance method for bifurvation analysis of large-scale mechanical systems," *Computer Methods in Applied Mechanics and Engineering*, vol. 296, pp. 18–38, 2015.